The HSSS Radical and the $HSSS^-$ Anion

Giulia de Petris,*,‡ Antonella Cartoni,‡ Marzio Rosi,§ and Anna Troiani‡

Dipartimento di Chimica e Tecnologie del Farmaco, Università "La Sapienza", Piazzale Aldo Moro 5, 00185 Rome, Italy, and Dipartimento di Ingegneria Civile ed Ambientale—Sezione Tecnologie Chimiche e Materiali per l'Ingegneria, ISTM-CNR—Università di Perugia, Via Duranti, I-06131, Perugia, Italy

Received: June 24, 2008

The HS_3 radical and the HS_3^- anion, the sulfur analogues of HO_3 and HO_3^-, have been detected for the first time by mass spectrometric experiments performed in the gas phase. The structural and energetic features of HS_3 and HS_3^- have been investigated by *ab initio* calculations. Both HS_3 and HS_3^- are characterized by HSSS open-chain structures, stable toward the dissociation into S_2 and $HS^{0/-}$. HS_3 adds to HS and HS_2 as the known HS_n species, and HS_3^- is the conjugate base of a strong Brønsted acid, the trisulfane HSSSH.

Introduction

The mercapto and thiosulfeno radicals, HS and HS_2, are the only known HS_n species. Likewise, HS_2^- is the only observed HS_n^- anion with $n > 1$,[1] likely due to the difficulty of preparing and separating the corresponding acids, the inorganic sulfanes H_2S_n.[2] By contrast, several HS_n^+ cations are known. For instance, the gas-phase basicity of S_6 and S_8 has been determined by mass spectrometric techniques,[3] and many HS_n^+ ions ($n = 1-9$) have been recently detected by H_2S or elemental sulfur chemical ionization.[4,5a]

As a part of our research along this line,[5] we report herein the first detection of the HS_3 radical and its HS_3^- anion, as isolated species in the gas phase. This new addition to prototypes of sulfur-containing species may be of interest to problems related to atmospheric and biochemical processes. Sulfur is one of the most abundant second-row elements in space, and new sulfur molecules and ions may be potentially relevant to the sulfur-driven chemistry of interstellar space and planetary atmospheres, as Io and Venus for example, where thiozone S_3 and sulfanes H_2S_n have been suggested to play significant roles.[6] In addition, sulfur is in the active sites of biological molecules, and cell regulation functions have been proposed for compounds containing "sulfane sulfur" atoms.[7] The interest in HS_3^- and its reactivity is also motivated by the high gas-phase acidity of trisulfane H_2S_3, possibly involved in corrosion processes occurring in sour gas deposits.[8]

The structure and stability of the $HS_3^{0/+/-}$ species involved in these experiments have been investigated by mass spectrometric techniques and ab initio calculations, also in comparison to the oxygen analogues HO_3[9,10] and HO_3^-,[11,12] and other sulfur analogues.[5a] The structural and energetic properties of these small reactive radicals and ions can help to understand their role in elementary processes, biochemical modifications and organic synthesis.[13]

Experimental Section

A. Mass Spectrometric Methods. All experiments were performed using a modified ZABSpec oa-TOF instrument (VG Micromass) described elsewhere.[14] Briefly, the instrument has a EBE-TOF configuration, where E, B stand for electric and magnetic sectors and TOF for orthogonal time-of-flight mass spectrometer. It is fitted with a modified EI—CI (electron ionization—chemical ionization) ion source and five collision cells. Typical operating conditions were as follows: accelerating voltage, 8 keV; source temperature, 423 K; repeller voltage, 0 V; emission current, 1 mA; nominal electron energy, 50 eV; source pressure, ca. 0.1—0.15 Torr, as read inside the source block by a Magnehelic differential pressure gauge. To identify isobaric components in the precursor ion, high-resolution CI mass spectra were recorded at 15000 fwhm (full width at half-maximum), corresponding to 67 ppm. The CAD (collisionally activated dissociation) spectra were recorded at 8 keV in a gas cell located after the magnet in the second field-free region. The CAD/TOF spectra of mass- and energy-selected ions were recorded at 0.8 keV in a gas cell located in the TOF sector. In the CAD experiments, helium was utilized as the target gas in the collision cell; the pressure was chosen to provide 80% transmittance.

The neutralization—reionization (NR) experiments[15] were performed in the pair of cells located after the magnet in the second field-free region of the instrument (8 keV). The experiments involve two subsequent charge-exchange processes occurring in a reduction—oxidation ($^+NR^+$) or reduction—reduction ($^+NR^-$) sequence. In the first step the mass-selected cation is reduced in the first cell by collision with Xe. All ions are removed at the exit of the cell by a pair of high-voltage deflecting electrodes. A beam containing only neutrals enters the second cell, where it is either oxidized by collision with O_2 ($^+NR^+$) or reduced by collision with Xe ($^+NR^-$). No signal was obtained by switching the deflector on in the absence of the reionizing gas. The vertical, one-electron charge-exchange processes occur on the femtosecond time scale; in each sequence they are separated by a microsecond time scale which corresponds to the time necessary to travel from the first to the second cell. The neutral molecules are reionized provided that they survive for this time. The detection of intact neutral species is proved by detection of a "recovery" peak at the same *m*/*z* ratio as the original ion. Charge reversal ($^+CR^-$) experiments are performed in only one collision cell where the positive ion undergoes a two-electron reduction (collision gas Xe). Gas pressures were set to achieve a beam transmittance of 80—90%, under near-single collision conditions. All NR and CR spectra were averaged over 100 acquisitions to improve the signal-to-

‡ Università "La Sapienza".
§ ISTM-CNR—Università di Perugia.

10.1021/jp8055637 CCC: $40.75
Published on Web 08/15/2008

noise ratio. The recovery peak of the $^{+}NR^{+}$ spectra was further analyzed in the TOF sector, and the CAD/TOF spectrum was compared to that of the precursor ions.

A possible isobaric contribution to the HS_3^+ precursor ion (*m*/*z* 97) is the $^{33}SSS^+$ isotopomer of the molecular ion S_3^+ (*m*/*z* 96). By high-resolution CI spectra and measurements of I/I^+ neutralization efficiency, this contribution is evaluated ≤0.47% of the precursor ion and ≤0.7% of the recovery peak. Any contamination is conclusively eliminated by using elemental ^{34}S in H_2/CI, where the $H^{34}S_3^+$ ion is not affected by isotopomers of S_3^+.

B. Materials. The chemicals were research-grade products with the following stated purity: HgS (Aldrich, 99.999 mol %), elemental sulfur-S (Aldrich, 99.998 mol %), elemental sulfur-^{34}S (Aldrich, 99.5% ^{34}S atoms). All other chemicals were research-grade products with a stated purity in excess of 99.95 mol %. Elemental sulfur and HgS were introduced through a direct insertion probe and heated in vacuo at 400 and 650 K, respectively. The S_3^+ signal was maximized in the EI spectrum of HgS by heating HgS at temperatures >600 K.

C. Computational Methods. The potential energy surfaces of HS_3^+, HS_3 and HS_3^- were investigated localizing the lowest stationary points at the B3LYP[16] level of theory in conjunction with the correlation consistent valence polarized set aug-cc-pVTZ,[17] augmented with a tight *d* function with exponent 2.457 for the sulfur atoms[18] to correct for the core polarization effects.[19] The basis set is denoted aug-cc-pV(T+*d*)Z.[20] At the same level of theory we computed the harmonic vibrational frequencies in order to check the nature of the stationary points, i.e. minimum if all the frequencies are real, saddle point if there is one, and only one, imaginary frequency. The energy of all the stationary points was computed at the higher level of calculation CCSD(T)[21] using the same basis set aug-cc-pV(T+*d*)Z. Both the B3LYP and the CCSD(T) energies were corrected to 298.15 K by adding the zero point energy correction computed using the scaled harmonic vibrational frequencies evaluated at B3LYP/aug-cc-pV(T+*d*)Z level and the thermal correction computed at the same level of theory. Selected geometry optimizations were performed also at the B3LYP level using the 6-311++G(2*d*,2*p*) and the 6-311++G(3*df*,3*pd*) basis sets;[22] at the MP2 level[23] with the aug-cc-pV(T+*d*)Z basis set; at the CCSD(T) level with the 6-311++G(2*d*,2*p*) basis set; at the CASSCF level[24] with the aug-cc-pV(T+*d*)Z basis set considering as active space all the valence orbitals occupied by all the valence electrons, that is 13 orbitals with 19 electrons for the HS_3 system. Thermochemical calculations were performed at both the CBS-Q[25] and W1[26] levels of theory. We recall that in the CBS-Q method the geometry optimization is performed at the MP2(FC)/6-31G$^+$ level, while the frequencies are evaluated at the UHF/6-31G† level. The energies are computed at the UMP2/6-311+G(3*d*2*f*,2*df*,2*p*), at the MP4(SDQ)/6-31+G(*d*(*f*),*p*) and at the QCISD(T)/6-31+G$^+$ level of theory. In the more accurate but more expensive W1 method the geometry optimization and the evaluation of the frequencies are performed at the B3LYP/VTZ + *d* level while the energies are computed at the CCSD(T)/AVDZ + 2*d*, CCSD(T)/AVTZ + 2*d*1*f*, and CCSD/AVQZ + 2*d*1*f* levels of theory (AV*n*Z is for aug-cc-pV*n*Z with *n* = D, T, Q). All calculations were performed using Gaussian 03,[27] and the analysis of the vibrational frequencies was performed using Molekel.[28]

Results and Discussion

Formation of HS_3 and HS_3^-. The experiments performed to produce the HS_3 radical and its anion rely on the preparation of suitable HS_3^+ ions, which primarily requires to assign the structure to the precursor cation and investigate the presence of isomeric species within the ionic population. The HS_3^+ ion was obtained by two different routes, using HgS and elemental sulfur as the source of sulfur clusters.

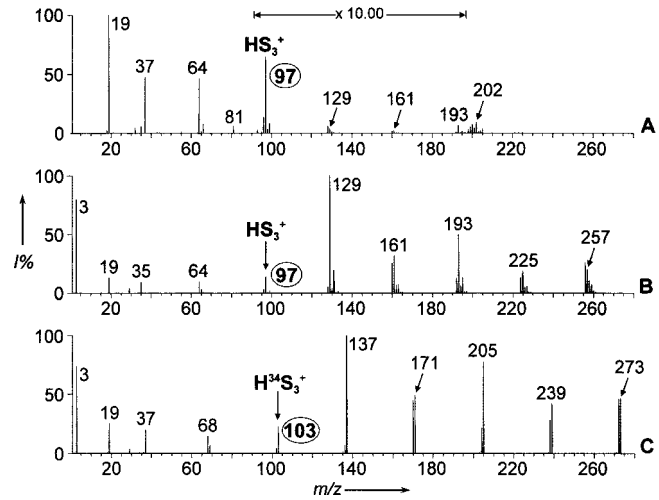

Figure 1. (A) CI spectrum of HgS/H_2O showing HS_3^+ (*m*/*z* 97), low abundance of HS_n^+ ions (n = 4−6, *m*/*z* 129, 161, 193) and the Hg^+ multiplet (*m*/*z* 202). (B) CI spectrum of elemental S/H_2 showing HS_3^+ (*m*/*z* 97) and HS_n^+ ions (n = 4−8). (C) CI spectrum of elemental ^{34}S/H_2 showing $H^{34}S_3^+$ (*m*/*z* 103) and $H^{34}S_n^+$ ions (n = 4−8). Note in addition in the low mass range: H_3^+ (*m*/*z* 3), H_3O^+ (*m*/*z* 19), H_3S^+ (*m*/*z* 35), $(H_2O)_2H^+$ (*m*/*z* 37) (A), $H_3{}^{34}S^+$ (*m*/*z* 37) (C), S_2^+ (*m*/*z* 64), $^{34}S_2^+$ (*m*/*z* 68), S_2OH^+ (*m*/*z* 81) (A). Trace water is always present in H_2/CI.

One route involves the proton transfer reaction from H_3O^+ to S_3, produced by high-temperature decomposition of HgS.

$$H_3O^+ + S_3 \rightarrow HS_3{}^+ + H_2O \qquad (1)$$

HgS vaporizes and decomposes giving Hg atoms and sulfur species, with a different composition compared to elemental sulfur.[29] The vapor produced by heating elemental sulfur contains in fact several S_n (n = 2−12) allotropes, whose composition depends on the pressure and temperature. In contrast, the vapor produced by decomposition of HgS is rich in lower S_n species, containing more than 80% of S_2 and minor fractions of S_3−S_6. Appearance potential measurements show that S_3^+ is formed by direct ionization of neutral S_3 in the HgS vapor.[29e] Consistent with this, a significant abundance of HS_3^+ (*m*/*z* 97) is obtained by HgS/H_2O chemical ionization (Figure 1A).

The $\Delta H°$ of reaction (1) is the difference between the proton affinity (PA) of H_2O and S_3. Thiozone in its ground state ($^1A_1$) has been theoretically and experimentally assigned a bent chain structure C_{2v}.[30,31] Protonation of the terminal and central sulfur atoms of S_3 thus gives ions of HSSS and SS(H)S connectivity, respectively. We have identified six minima on the singlet ($\mathbf{1}^+$−$\mathbf{4}^+$) and triplet ($^3\mathbf{5}^+$, $^3\mathbf{6}^+$) surfaces of HS_3^+ (Figure 2, Table 1S, Supporting Information), that correspond to the protonation products of the theoretically predicted S_3 species, namely the singlet S_3 C_{2v}, the singlet three-membered ring D_{3h} and the triplet C_{2v}.[30] Thus, $\mathbf{1}^+$, $\mathbf{2}^+$ and $^3\mathbf{5}^+$ are $HSSS^+$ ions from protonation of singlet and triplet S_3 C_{2v} on the terminal sulfur atom, whereas $\mathbf{4}^+$ and $^3\mathbf{6}^+$ are the less stable $SS(H)S^+$ forms protonated on the central sulfur atom.

As shown in Figure 2, the most stable HS_3^+ species is the singlet trans-planar $HSSS^+$ ion $\mathbf{1}^+$, in agreement with previous work on the singlet HS_3^+ ion.[4,32] In addition, the geometries of

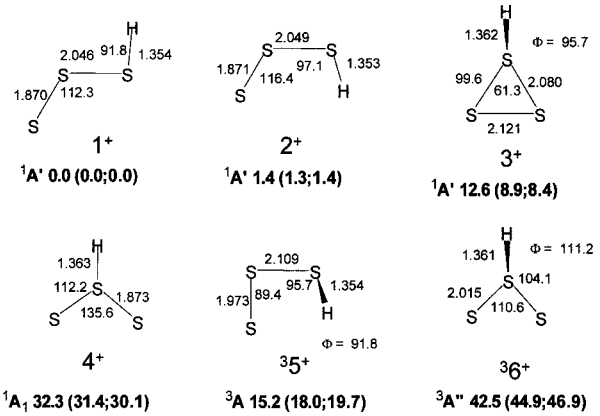

Figure 2. B3LYP optimized geometries and relative energies (kcal mol^{-1}) at 298.15 K of HS_3^+ ions, in parentheses CCSD(T) and W1 relative energies. Φ indicates the SSSH dihedral angles.

species $\mathbf{1}^+$, $\mathbf{2}^+$, and $\mathbf{3}^+$ are close to those previously reported by Wong et al.,[32c] optimized at the B3LYP/6-31G(2df,p) level. Our optimized geometry of S_3 (1.924 Å and 118.3°) is also in good agreement with the experimental values of 1.917(1) Å and 117.36°.[31] Further to this, the computed energy differences between the dissociation limits have been compared to the available experimental data,[29b,33,34] the best agreement being found with the W1 method.

The PA values of S_3 are 179.8 kcal mol^{-1} (CCSD(T)) and 178.1 kcal mol^{-1} (W1) (Table 1), the latter in better agreement with previously reported values of 178.2 and 178.6 kcal mol^{-1}.[32a,c] The PA values of the central sulfur atom are significantly lower and much closer to each other, 148.4 (CCSD(T)) and 148.0 (W1) kcal mol^{-1}, respectively, due to the slightly lower stability (1.3 kcal mol^{-1}) of ion $\mathbf{4}^+$ at the W1 level. An important feature of both the singlet and triplet surface is that the isomerization energy of $HSSS^+$ to $SS(H)S^+$ isomers, $\mathbf{1}^+ \rightarrow \mathbf{4}^+$, $^3\mathbf{5}^+ \rightarrow {}^3\mathbf{6}^+$, is close to or higher than the lowest dissociation limit of $\mathbf{1}^+$ and $^3\mathbf{5}^+$ (Table 1). This energy profile indicates that a pure population of $HSSS^+$ ions can be obtained under suitable experimental conditions.

Using H_3O^+ as the Brønsted acid, the reaction (1) forming the most stable ion $\mathbf{1}^+$ is computed to be exothermic by 13.2 kcal mol^{-1} (W1), in agreement with the experimental PA of H_2O (165 kcal mol^{-1}).[34] S_3 is hence protonated on the terminal sulfur atom, the formation of $\mathbf{4}^+$ being endothermic by ≈17 kcal mol^{-1}. A convincing clue to the failure to form ion $\mathbf{4}^+$ comes from S_2, whose PA (149.1 kcal mol^{-1})[32c] happens to be close to that of S_3 on the central sulfur atom. Despite the high partial pressure of S_2, no HS_2^+ ions are observed (Figure 1A). On the other hand, the energy deposited into HS_3^+ by reaction (1), also considering the energy partitioning between the products, is not sufficient to promote isomerization (Table 1).

The second route to the HS_3^+ ion is the chemical ionization of elemental sulfur and H_2 (Figure 1B). In such a case, the vapor is rich in higher S_n species and the exothermic protonation from H_3^+ promotes dissociation of HS_n^+ ions formed with excess energy.

$$H_3^+ + S_n \rightarrow HS_n^+ (+H_2) \rightarrow HS_3^+ + S_{n-3} + H_2 \qquad (2)$$

Consistent with this, the CAD spectra of HS_n^+ ions ($n = 5-7$) display HS_3^+ as the most abundant fragment. Also in this case, $HSSS^+$ ions are expected to form the largest part of the beam. The structural features of these HS_n^+ ions (branched rings $HS(S_{n-1})^+$ and open-chain HSS_{n-1}^+ isomers) indicate in fact that their dissociation yields ions of HSSS connectivity.[3,32c] In addition, the ring opening of cyclic ions $H(S_n)^+$ to singlet open-chain HSS_{n-1}^+ ions has been computed to be endothermic by only 5−10 kcal mol^{-1}.[32c] We computed at the CCSD(T) level the $\Delta H°$ of reaction (2) involving S_5, that amounts to −30.5 kcal mol^{-1}. Also in this case, taking into account the energy partitioning between the products, the excess energy of HS_3^+ is not expected to promote isomerization. The same holds for other S_n clusters, given the close PA values of S_5-S_8[32c] and $H_f°$ values of the S_2-S_4 molecules.[29d,34] Possible implications of dissociations into triplet $HSSS^+$ ions ($^3\mathbf{5}^+$) will be discussed later on. Finally, reaction (2) allows one to utilize elemental ^{34}S and rule out isobaric contaminations in NR experiments (Figure 1C).

The structure of the HS_3^+ and $H^{34}S_3^+$ ions obtained by reactions (1) and (2) was analyzed by CAD mass spectrometry. Their CAD spectra are indistinguishable (Figure 3A,B), showing the expected labeled and unlabeled fragments, S_3^+ (*m/z* 96, 102), HS_2^+ (*m/z* 65, 69), S_2^+ (*m/z* 64, 68), HS^+ (*m/z* 33, 35) and S^+ (*m/z* 32, 34). CAD spectra were also recorded at 0.8 keV in the TOF sector of the instrument (Figure 3C). They serve as reference spectra for the analysis of the neutral formed.

The HS_3^+ ions generated by reactions (1) and (2) were then submitted to neutralization. The $^+NR^+$ spectra of HS_3^+ and $H^{34}S_3^+$ show intense recovery peaks at *m/z* 97 and 103 (Figure 4). Both experiments prove that HS_3 is formed and survives for the minimum lifetime of 0.8 μs, as derived from the molecular weight of 97 Da and the accelerating voltage of 8 keV. The neutralization and reionization processes are reasonably considered vertical processes, as they occur on the femtosecond time scale. On this basis, the neutral must have the same structure as the precursor ion. The structure of the neutral was also directly probed by reanalyzing the "recovery" peak, that was separated from all other fragments and structurally analyzed in the TOF sector.

$$CAD \leftarrow HS_3^+ \xrightarrow{+e} HS_3 \xrightarrow{-e} HS_3^+ \rightarrow CAD$$

As shown in Figure 3, its NR-CAD spectrum (Figure 3D) is much the same as that of the precursor ion (Figure 3C), pointing to the formation of a radical having the HSSS connectivity and geometry of the ion $\mathbf{1}^+$. HS_3 may also be revealed by negative reionization, provided that an anion of strictly related structure can be formed and that the radical has sufficiently high electron affinity. Like the previous experiments, the $^+NR^-$ spectra of both HS_3^+ and $H^{34}S_3^+$ ions show intense recovery peaks at *m/z* 97 and 103 (Figure 5), that positively proves the existence of the hitherto unknown HS_3^- anion. Further to this, the HS_3^- ion is formed by $^+CR^-$ (charge reversal) experiments, that is by a two-electron reduction of HS_3^+ (see the inset of Figure 5B). As discussed in the next section, this finding indicates favorable Franck−Condon factors for the cation, neutral and anion surfaces.

Structures and Energies of HS_3 and HS_3^-. The structures of the minima identified on the doublet and quartet surfaces of HS_3 are reported in Figure 6, and the vibrational frequencies are reported in Table 1S. The species are denoted by the numbers used to indicate the connectivity and geometry of the cation, irrespective of their relative stability: e.g. **5** is the neutral having the connectivity HSSS and nonplanar geometry of the triplet cation $^3\mathbf{5}^+$.

Accordingly, the doublet **1** of HSSS connectivity and the ground-state $HSSS^+$ ion $\mathbf{1}^+$ have similar structures (Figures 2 and 6). Compared to $\mathbf{1}^+$, the HS−SS and HSS−S bonds of **1** are elongated by 0.090 and 0.068 Å, respectively, while the

TABLE 1: Energy Changes and Barrier Heights (kcal mol^{-1}, 298.15 K) Computed at the B3LYP/aug-cc- pV(T+*d*)Z, CCSD(T)/aug-cc-pV(T+*d*)Z, W1 and CBS-Q Levels of Theory for Selected Dissociation and Isomerization Processes of HS_3^+, HS_3 and HS_3^-[a]

	ΔH				barrier height	
	B3LYP	CCSD(T)	W1	CBS-Q	B3LYP	CCSD(T)
HS_3^+						
$\mathbf{1}^+ \rightarrow S_2^+ + HS$	56.0	55.1	58.8	60.6		
$\mathbf{4}^+ \rightarrow S_3^+ + H$	53.9	54.4	55.9	54.1		
$^3\mathbf{5}^+ \rightarrow S_2^+ + HS$	40.8	37.1	39.1	39.0		
$\mathbf{1}^+ \rightarrow S_3 + H^+$	180.7	179.8	178.1	178.1		
$\mathbf{1}^+ \rightarrow \mathbf{2}^+$	1.4	1.3	1.4	1.7	14.5	15.9
$\mathbf{1}^+ \rightarrow \mathbf{4}^+$	32.3	31.4	30.1	31.5	58.8	57.8
$^3\mathbf{5}^+ \rightarrow {}^3\mathbf{6}^+$	27.3	26.9	27.2	27.9	42.8	44.4
$\mathbf{1}^+ \rightarrow \mathbf{3}^+$	12.6	8.9	8.4	10.3	34.4	38.0
$\mathbf{2}^+ \rightarrow \mathbf{3}^+$	11.2	7.6	7.0	8.6	32.6	23.0
HS_3						
$\mathbf{5} \rightarrow S_2 + HS$	32.5	33.6	36.8	37.2		
$\mathbf{5} \rightarrow HS_2 + S$	61.3	59.5	64.1	64.8		
$\mathbf{6} \rightarrow S_3 + H$	33.9	29.6	29.8	30.3		
$\mathbf{5} \rightarrow \mathbf{6}$	28.5	30.4	29.2	28.1	41.5	42.6
HS_3^-						
$\mathbf{5}^- \rightarrow S_2(^1\Delta_g)^b + HS^-$	42.0	45.5	47.7	48.2		
$\mathbf{5}^- \rightarrow S_2^- + HS$	43.7	47.0	50.0	50.4		
$\mathbf{6}^- \rightarrow S_3^- + H$	42.7	46.0	46.7	44.3		
$^3\mathbf{1}^- \rightarrow S_2 + HS^-$	15.6	11.4	11.6	15.8		
$^3\mathbf{1}^- \rightarrow {}^3\mathbf{2}^-$	−0.4	−0.6	−0.6	0.2	<0.5	<0.5
$\mathbf{5}^- \rightarrow \mathbf{6}^-$	10.2	9.5	8.7	9.7	28.2	28.3
$^3\mathbf{1}^- \rightarrow {}^3\mathbf{4}^-$	26.7	24.6	22.5	*c*	38.2	33.9

[a] Unless stated otherwise, the dissociation products are all considered in their ground state. [b] The singlet−triplet difference of 13.4 kcal mol^{-1} has been added to ΔH.[35] [c] $^3\mathbf{4}^-$ is not a minimum at the CBS-Q level.

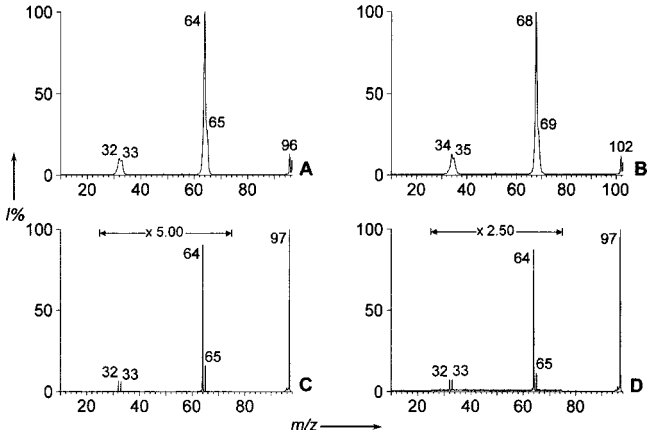

Figure 3. (A) CAD spectrum of HS_3^+ (*m*/*z* 97) from HgS/H_2O CI. (B) CAD spectrum of $H^{34}S_3^+$ (*m*/*z* 103) from elemental ^{34}S/H_2 CI. The parent ions at *m*/*z* 97 and 103 are out of the mass range. (C) CAD/TOF spectrum of HS_3^+ from HgS/H_2O CI. (D) NR-CAD mass spectrum of the HS_3^+ recovery peak from $^+NR^+$. Accelerating voltage: 8 keV (A) and (B); 0.8 keV (C) and (D).

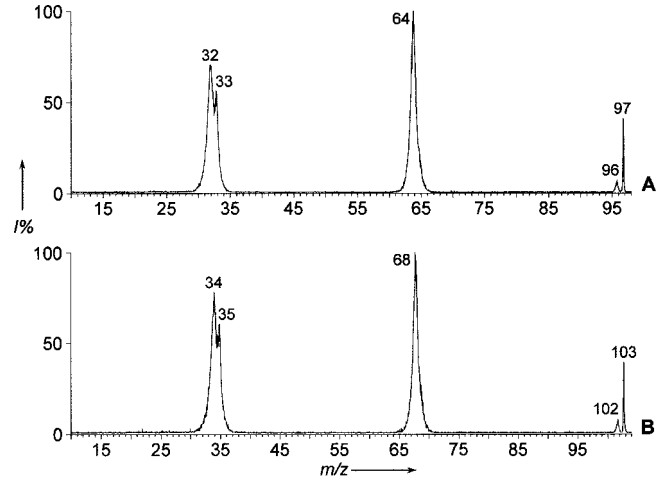

Figure 4. $^+NR^+$ spectra of (A) HS_3^+ and (B) $H^{34}S_3^+$. Note the recovery peaks at *m*/*z* 97 and 103. Peaks at *m*/*z* 65 and 69 are unresolved.

H−SSS bond is shortened by 0.008 Å. As shown in Figure 6, the ground state on the neutral surface is the doublet **5** with the hydrogen atom out of the S_3 plane. It is slightly more stable than **1** at all levels of theory except at the CBS-Q level, where **5** is found to be less stable than **1** by only 0.3 kcal mol^{-1}. Moreover, the barrier for the **1** → **5** isomerization is only 0.08 and 0.05 kcal mol^{-1} at the B3LYP/aug-cc-pV(T+*d*)Z and MP2/aug-cc-pV(T+*d*)Z levels, respectively; this barrier disappears with the inclusion of the ZPE correction.

The global minimum is of major interest to the experiments reported here, hence the geometries of **5** and **1** were optimized at different levels of theory. The results are reported in Table 2 and show that the nonplanar structure **5** is slightly more stable than the trans-planar **1** at all levels of calculation. Notably, quite close optimized geometries are obtained at the CCSD(T) and B3LYP levels with the same basis set (6-311++G(2d,2p)). Likewise, the **1** → **5** relative energies computed at the CCSD(T)/6-311++G(2d,2p) level on CCSD(T) and B3LYP optimized geometries are very close (1.4 and 1.3 kcal mol^{-1}, Table 2). Finally, we optimized the geometry of **1** at CCSD(T)/aug-cc-pV(T+*d*)Z level ($r(S_1S_2) = 1.942$ Å, $r(S_2S_3) = 2.120$ Å, $r(S_3H) = 1.344$ Å, $\angle S_1S_2S_3 = 106.2°$, $\angle S_2S_3H = 92.7°$); the bond lengths are close to those obtained at B3LYP level with the same basis set, and the energy of **1** is lowered by only 0.09 kcal mol^{-1}.

Similar to the cation, the radical **6** of SS(H)S connectivity is ca. 30 kcal mol^{-1} less stable than HSSS **5** (29.2 kcal mol^{-1} (W1), 30.4 kcal mol^{-1} (CCSD(T)), and also the barrier for the **5** → **6** isomerization exceeds the lowest dissociation limit of **5** (Table 1). The HSSS radical is thus experimentally detectable

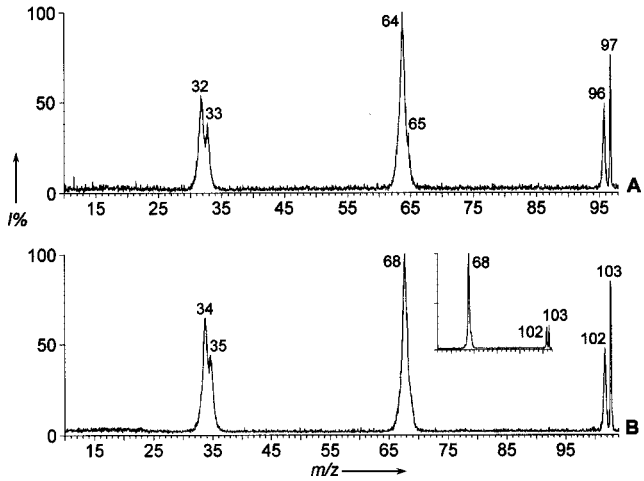

Figure 5. $^+NR^-$ spectra of (A) HS_3^+ and (B) $H^{34}S_3^+$. Note the recovery peaks corresponding to HS_3^- (*m/z* 97) and $H^{34}S_3^-$ (*m/z* 103). The inset shows the $^+CR^-$ spectrum of $H^{34}S_3^+$ (*m/z* 103).

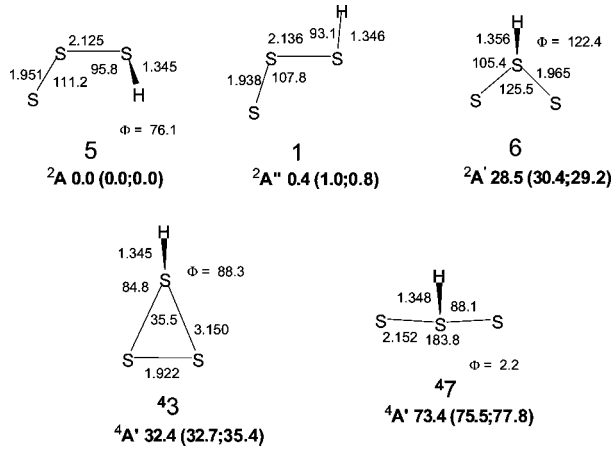

Figure 6. B3LYP optimized geometries and relative energies (kcal mol^{-1}) at 298.15 K of HS_3 species, in parentheses CCSD(T) and W1 relative energies. Φ indicates the SSSH dihedral angles.

in the absence of isomeric species, provided that it is formed below the dissociation energy. Due to the vertical nature of the neutralization, the neutral species is in fact generated with excess internal energy, which is the difference between the adiabatic and vertical recombination energy of the precursor ion. In such a case, **5** is predicted to be generated from ion $\mathbf{1}^+$ with the excitation energy of 4.1 kcal mol^{-1} (CCSD(T), Table 3), far below the lowest dissociation energy into S_2 and HS, 33.6 kcal mol^{-1} (CCSD(T)) and 36.8 kcal mol^{-1} (W1).

The dissociation limit S_3 + H is higher in energy, and the experimental $\Delta H°$ for the reaction S_2 + HS → S_3 + H is 21.9 ± 2.2 kcal mol^{-1}.[33] The computed $\Delta H°$ values are as follows: $\Delta H°_{CCSD(T)}$ = 26.4 (aug-cc-pV(T+*d*)Z) and 25.4 (6-311+G(3df,2p)), respectively, $\Delta H°_{W1}$ and $\Delta H°_{CBS\text{-}Q}$ = 21.2 and 22.2 kcal mol^{-1}, respectively. Compared to $\Delta H°_{exp}$, the CCSD(T) values thus differ by more than the experimental error bar, whereas the CBS-Q and W1 values are largely within the error limits. Despite these differences, the low excitation energy of **5** indicates that HSSS is formed largely below the dissociation and isomerization barriers. This prediction is consistent with the experimental evidence, showing no difference between the starting and final ionic population, that is the HS_3^+ precursor ion and the "recovery" HS_3^+ ion.

It must be noted that, although **5** is the lowest energy minimum, a true equilibrium structure cannot be assigned due to the flatness of the surface. Interestingly, **5** would also be generated from the triplet ion $^3\mathbf{5}^+$, whereas no neutral counterpart of ion $\mathbf{3}^+$ was identified by our calculations on the doublet surface. The ring structure is in fact only stabilized in the singlet cation $\mathbf{3}^+$. The ring-like quartet $^4\mathbf{3}$ is close to the lowest dissociation limit; the anion $^3\mathbf{3}^-$ was not found at W1 level (Figures 6 and 7), whereas at B3LYP/aug-cc-pV(T+*d*)Z level, it is a complex that correlates with the higher dissociation limit S_2^- + HS.

Figure 7 and Table 1S report the structures and vibrational frequencies of the six minima identified on the singlet ($\mathbf{5}^-$, $\mathbf{6}^-$) and triplet ($^3\mathbf{1}^-$–$^3\mathbf{4}^-$) surfaces of HS_3^-. The geometry of the most stable $HSSS^-$ anion $\mathbf{5}^-$ compares quite well with previous G2 calculations.[8a] Its structure is close to that of the radical **5**, the bond length difference being ≤0.09 Å. As a consequence, the vertical excitation energy of the singlet anion $\mathbf{5}^-$ formed from **5** is predicted to be only 2.0 kcal mol^{-1} (Table 3), consistent with the experimental evidence. Different from the cation and neutral surfaces, the barrier to the $HSSS^- \rightarrow SS(H)S^-$ isomerization ($\mathbf{5}^- \rightarrow \mathbf{6}^-$) lies below the lowest dissociation limit into HS^- and $S_2(^1\Delta_g)$ (Table 1), though far above the vertical excitation energy of $\mathbf{5}^-$. Notably, a good agreement with experimental data is observed here using both the CCSD(T) and W1 methods. For instance, $\Delta H°_{exp}$ of the reaction S_2 + $HS^- \rightarrow S_3^-$ + H = 22.1 ± 3.2 kcal mol^{-1},[33,34,36] $\Delta H°_{CCSD(T)}$ = 23.4 (aug-cc-pV(T+d)Z) and $\Delta H°_{W1}$ = 21.1 kcal mol^{-1}.

The vertical reduction of HS_3 does not prove to be a viable route to the triplet $HSSS^-$ anion ($^3\mathbf{1}^-$), characterized by a long central S−S bond (2.967 Å). The ion would be formed with an excitation energy of 24.8 kcal mol^{-1}, well above the dissociation energy into HS^- and $S_2(^3\Sigma_g^-)$ that is only 11.6 kcal mol^{-1} above $^3\mathbf{1}^-$. Interestingly, the triplet $HSSS^-$ ion is structurally similar to the triplet HO_3^- anion, a weakly bound complex with a very long HO−OO bond (2.613 Å).[12b] The singlet HS_3^- and HO_3^- anions are instead rather different. In fact, the geometrical features of the neutral and charged HS_3 and HO_3 species show that the overlap between the cation, neutral and anion surfaces is much better in the $HS_3^{+/0/-}$ than in the $HO_3^{+/0/-}$ system. For instance, the HS−SS bond length ranges from 2.046 to 2.148 Å in the $HS_3^{+/0/-}$ species, whereas the HO−OO bond length ranges from 1.384 to 1.857 Å in the $HO_3^{+/0/-}$ species,[9c,10,12,37] due to the small π character of the interaction in HO_3^- and also in HO_3. Consistent with this, HS_3^- is expected to be formed by a two-electron reduction of HS_3^+, whereas the opposite is true for HO_3^-. This peculiarity is confirmed by the experimental evidence. As shown, the $^+CR^-$ spectrum of HS_3^+ displays a recovery peak corresponding to HS_3^- (Figure 5B), whereas under the same conditions HO_3^+ is not reduced to the HO_3^- anion, whose dissociation energy (15.4 kcal mol^{-1})[12] is also lower than that of HS_3^-. Accordingly, HO_3^- is only detectable by the two-step process occurring in $^+NR^-$ experiments.[11]

Further differences are evidenced in the simplified Scheme 1, that shows the H addition reactions to the valence-shell isoelectronic X_3 species (X_3 = O_3, S_3, S_2O, SO_2). HS_3 is the missing link in the family of the HX_3 reaction intermediates. The sulfur species are all more stable toward the dissociation than HO_3, which is weakly bound with respect to the HO and O_2 products.[10] As a result of the hydrogen atom addition to S_3, the (H)S−SS bond length is elongated going from 1.917 Å in S_3[31] to 2.125 Å in HS_3 (Δ = 0.208 Å), which is 0.07 Å longer than a single S−S bond (e.g., 2.056 in HSSH).[34] The same holds for the (H)O−SS and (H)O−SO radicals, where the central O−S bonds are 0.2 Å longer than those of S_2O and SO_2.[5a,34,38] The effect is instead dramatic in HO_3, whose structure and bonding

TABLE 2: Optimized Geometries (Å and deg) and Relative Energies (kcal mol^{-1}, 298.15 K) of Species 5 and 1 Computed at Various Levels of Theory[a]

	B3LYP/B1	B3LYP/B2	B3LYP/B3	MP2/B1	CASSCF/B1	CCSD(T)/B3
5						
$r(S_1S_2)$	1.951	1.949	1.970	1.929	1.983	1.988
$r(S_2S_3)$	2.125	2.124	2.147	2.092	2.139	2.147
$r(S_3H)$	1.345	1.346	1.345	1.338	1.356	1.339
$\angle S_1S_2S_3$	111.2	111.4	111.0	109.7	110.2	109.7
$\angle S_2S_3H$	95.8	95.8	95.4	94.8	96.4	94.7
$\angle S_1S_2S_3H$	76.1	75.4	77.1	82.6	82.6	81.2
1						
$r(S_1S_2)$	1.938	1.935	1.956	1.914	1.964	1.970
$r(S_2S_3)$	2.136	2.135	2.159	2.094	2.160	2.162
$r(S_3H)$	1.346	1.346	1.346	1.340	1.356	1.340
$\angle S_1S_2S_3$	107.8	108.0	107.8	106.4	107.2	106.6
$\angle S_2S_3H$	93.1	92.8	92.7	92.9	93.1	92.0
$\angle S_1S_2S_3H$	180.0	180.0	180.0	180.0	180.0	180.0
ΔH_{298} **5** → **1**	0.4 (1.0)[b]	0.5	0.6	0.9	1.4	1.4 (1.3)[c]

[a] B1 = aug-cc-pV(T+*d*)Z basis set, B2 = 6-311++G(3df,3pd) basis set, B3 = 6-311++G(2d,2p) basis set. [b] In parentheses CCSD(T)/B1 energy computed on B3LYP/B1 geometry. [c] In parentheses CCSD(T)/B3 energy computed on B3LYP/ B3 geometry

TABLE 3: Vertical Excitation Energies of HS_3 at the Geometry of the HS_3^+ Cation in Parentheses and of HS_3^- at the Geometry of HS_3 and HS_3^+ in Parentheses

species	B3LYP/aug-cc-pV(T+*d*)Z	CCSD(T)/aug-cc-pV(T+*d*)Z
HS_3		
1 (**1**$^+$)	3.2	3.2
5 (**1**$^+$)	3.6	4.1
1 (**2**$^+$)	3.9	3.8
5 (**2**$^+$)	4.3	4.8
5 (^{3}**5**$^+$)	13.1	11.3
HS_3^-		
5$^-$ (**5**)	2.2	2.0
5$^-$ (**1**)	8.6	8.3
^{3}**1**$^-$ (**1**)	28.2	24.8
5$^-$ (**1**$^+$)	18.0	17.7
5$^-$ (**2**$^+$)	17.8	17.4
5$^-$ (^{3}**5**$^+$)	15.3	13.5

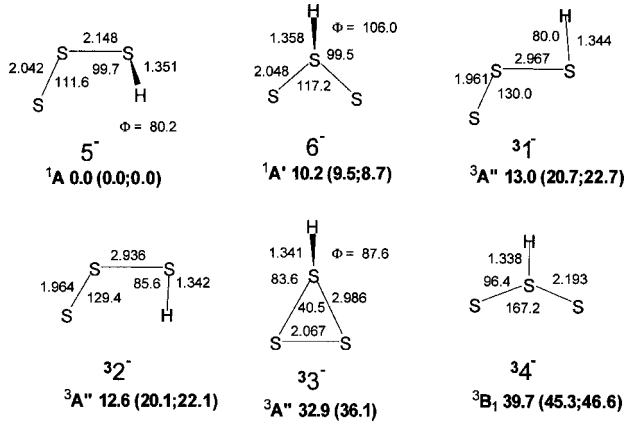

Figure 7. B3LYP optimized geometries and relative energies (kcal mol^{-1}) at 298.15 K of HS_3^- ions, in parentheses CCSD(T) and W1 relative energies. Φ indicates the SSSH dihedral angles.

have been extensively investigated.[9c,10] Here the (H)O−OO bond length goes from 1.278 Å in O_3[34] to 1.688 Å,[9c] much longer than a single O−O bond (e.g., 1.475 in HOOH).[34] The H atom addition to X_3 thus modifies the bonding in a rather similar manner with the exception of HO_3, showing the major role of sulfur in the bonding stabilization.

In summary, the reported results positively demonstrate the existence of HS_3 and HS_3^- as isolated species in the gas phase. The low recombination energy of $HSSS^+$, 8.40 eV, and the high

SCHEME 1: Simplified Energy Profiles Relevant to HX_3 Species ($X_3 = S_3, O_3, S_2O, SO_2$)

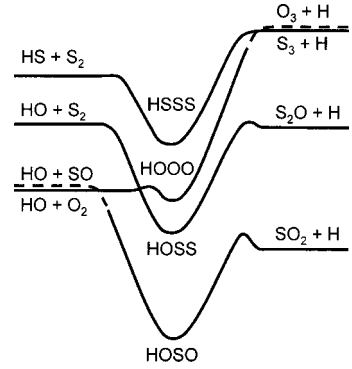

electron affinity of HSSS, 2.17 eV, make these species good candidates for recombination reactions of potential atmospheric interest. In addition, HS_3^- is the conjugate base of the Brønsted acid H_2S_3, whose computed gas-phase acidity, 327.7 kcal mol^{-1},[8] is comparable to that of HCl (328.1 kcal mol^{-1}) or bromoacetic acid (328.2 kcal mol^{-1}).[39] Among the HX_3 species of Scheme 1, HS_3 and HO_3 are the only intermediates of exothermic H-addition reactions to S_3 and O_3, respectively. HO_3[9] is the transient intermediate of atmospherically relevant reactions, and other processes such as the ozonation of C−H bonds and antibody-catalyzed chemical modification of antigens.[13] In particular, the reaction H + O_3 → O_2 + HO produces highly vibrationally excited HO(v) radicals, relevant to the terrestrial airglow and the "ozone deficit problem".[13a,b] The reaction H + S_3 → S_2 + HS is among the H-addition reactions included in atmospheric models of the lower atmosphere of Venus.[6c] The reaction would be worthy of further investigation, as it has been suggested that thiozone could play a role, in the subcloud venusian atmosphere, similar to that of ozone in the Earth's upper atmosphere.[13a]

Conclusions

The first experimental detection of the HS_3 radical and HS_3^- anion has been reported. The experimental and computational study of $HS_3^{+/0/-}$ species, using mass spectrometric techniques and ab initio calculations, allows the assignment of open-chain bent structures of HSSS connectivity to the new species identified. HSSS has been prepared by collisional electron transfer to $HSSS^+$; the

$HSSS^-$ anion, the conjugate base of trisulfane H_2S_3, has been prepared by collisional electron transfer to HSSS.

Acknowledgment. Financial support by the Italian Government (PRIN) and Rome University "La Sapienza" is gratefully acknowledged. The authors thank Stefania Recaldin for editorial assistance.

Supporting Information Available: This material is available free of charge via the Internet at http://pubs.acs.org.

References and Notes

(1) (a) Moran, S.; Ellison, G. B. *J. Phys. Chem.* **1988**, *92*, 1794. (b) O' Hair, R. A. J.; DePuy, Ch. H.; Bierbaum, V. M. *J. Phys. Chem.* **1993**, *97*, 7955.

(2) (a) Feher, F.; Laue, W.; Winkhaus, G. *Z. Anorg. Allg. Chem.* **1956**, *288*, 113. (b) Feher, F.; Winkhaus, G. *Z. Anorg. Allg. Chem.* **1956**, *288*, 123.

(3) Abboud, J.-L. M.; Essefar, M.; Herreros, M.; Mò, O.; Molina, M. T.; Notario, R.; Yáñez, M. *J. Phys. Chem. A* **1998**, *102*, 7996.

(4) Ligon, A. P.; Gab, S. *Int. J. Mass Spectrom.* **2005**, *243*, 241.

(5) (a) de Petris, G.; Rosi, M.; Troiani, A. *J. Phys. Chem. A* **2007**, *111*, 6526. (b) de Petris, G.; Rosi, M.; Troiani, A. *Chem. Commun.* **2006**, 4416. (c) de Petris, G. *Acc. Chem. Res.* **2002**, *35*, 305. (d) Cacace, F.; Cipollini, R.; de Petris, G.; Rosi, M.; Troiani, A. *J. Am. Chem. Soc.* **2001**, *123*, 478.

(6) (a) Bohme, D. K.; Herbst, E.; Kaifu, N.; Saito, S. *Chemistry and Spectroscopy of Interstellar Molecules*; University of Tokyo Press: Tokyo, 1992. (b) Bettens, R. P. A.; Lee, H.-H.; Herbst, E. *Astrophys. J.* **1995**, *443*, 664. (c) Krasnopolsky, V. A. *Icarus* **2007**, *191*, 25. (d) Moses, J. I.; Zolotov, M. Y.; Fegley, B., Jr *Icarus* **2002**, *156*, 76. (e) Spencer, J. R.; Jessup, K. L.; McGrath, M. A.; Ballester, G. E.; Yelle, R. *Science* **2000**, *288*, 1208. (f) Fegley, B., Jr.; Molotov, M. Y.; Lodders, K. *Icarus* **1997**, *125*, 416. (g) Prinn, R. G. *Geophys. Res. Lett.* **1979**, *6*, 807.

(7) Toohey, J. I. *Biochem. J.* **1989**, *264*, 625.

(8) (a) Otto, A. H.; Steudel, R. *Eur. J. Inorg. Chem.* **1999**, 2057. (b) Steudel, R. *Top. Curr. Chem.* **2003**, *231*, 99.

(9) (a) Cacace, F.; de Petris, G.; Pepi, F.; Troiani, A. *Science* **1999**, *285*, 81. (b) Nelander, B.; Engdahl, A.; Svensson, T. *Chem. Phys. Lett.* **2000**, *332*, 403. (c) Suma, K.; Sumiyoshi, Y.; Endo, Y. *Science,* **2005**, *308*, 1885. (d) Cooper, P. D.; Moore, M. H.; Hudson, R. L. *J. Phys. Chem. A* **2006**, *110*, 7985. (e) Murray, C.; Derro, E. L.; Sechler, T. D.; Lester, M. I. *J. Phys. Chem. A* **2007**, *111*, 4727. See also: (f) Speranza, M. *Inorg. Chem.* **1996**, *35*, 6140.

(10) (a) Dupuis, M.; Fitzgerald, G.; Hammond, B.; Lester, W. A.; Schaefer, H. F., III *J. Chem. Phys.* **1986**, *84*, 2691. (b) Setokuchi, O.; Sato, M.; Matuzawa, S. *J. Phys. Chem. A* **2000**, *104*, 3204. (c) Varandas, A. J. C. *Int. Rev. Phys. Chem.* **2000**, *19*, 199. (d) Yu, H. G.; Varandas, A. J. C. *Chem. Phys. Lett.* **2001**, *334*, 173. (e) Fabian, W. M. F.; Kalcher, J.; Janoschek, R. *Theor. Chem. Acc.* **2005**, *114*, 182. (f) Mansergas, A.; Anglada, J. M.; Olivella, S.; Ruiz-Lopez, M. F.; Martins-Costa, M. *Phys. Chem. Chem. Phys.* **2007**, *9*, 5865.

(11) Cacace, F.; Cipollini, R.; de Petris, G.; Troiani, A. *Int. J. Mass Spectrom.* **2003**, *228*, 717.

(12) (a) Koller, J.; Plesničar, B. *J. Am. Chem. Soc.* **1996**, *118*, 2470. (b) Kraka, E.; Cremer, D.; Koller, J.; Plesničar, B. *J. Am. Chem. Soc.* **2002**, *124*, 8462. (c) Mazziotti, D. A. *J. Phys. Chem. A* **2007**, *111*, 12635.

(13) (a) Wayne, R. P. *Chemistry of Atmospheres*; Clarendon Press: Oxford, 2000. (b) Varandas, A. J. C. *ChemPhysChem* **2002**, *3*, 433. (c) Cerkovnik, J.; Erěn, E.; Koller, J.; Plesničar, B. *J. Am. Chem. Soc.* **2002**, *124*, 404. (d) Wentworth, P., Jr.; Wentworth, A. D.; Zhu, X.; Wilson, I. A.; Janda, K. D.; Eschenmoser, A.; Lerner, R. A. *Proc. Natl. Acad. Sci. U.S.A.* **2003**, *100*, 1490. (e) Plesničar, B.; Cerkovnik, J.; Tuttle, T.; Kraka, E.; Cremer, D. *J. Am. Chem. Soc.* **2002**, *124*, 11260.

(14) Bernardi, F.; Cacace, F.; de Petris, G.; Pepi, F.; Rossi, I.; Troiani, A. *Chem. Eur. J.* **2000**, *6*, 537–544.

(15) (a) Holmes, J. L. *Mass Spectrom. Rev.* **1989**, *8*, 513. (b) Schalley, C. A.; Hornung, G.; Schröder, D.; Schwarz, H. *Chem. Soc. Rev.* **1998**, *27*, 91. (c) Tureček, F. *Theory and Ion Chemistry, The Encyclopedia of Mass Spectrometry, Vol. 1*; Armentrout, P. R., Ed.; Elsevier: New York, 2003.

(16) (a) Becke, A. D. *J. Phys. Chem.* **1993**, *98*, 5648. (b) Stephens, P. J.; Devlin, F. J.; Chablowski, C. F.; Frisch, M. J. *J. Phys. Chem.* **1994**, *98*, 11623.

(17) (a) Dunning, T. H., Jr *J. Chem. Phys.* **1989**, *90*, 1007. (b) Woon, D. E.; Dunning, T. H., Jr *J. Chem. Phys.* **1993**, *98*, 1358. (c) Kendall, R. A.; Dunning, T. H., Jr.; Harrison, R. J. *J. Chem. Phys.* **1992**, *96*, 6796.

(18) Bauschlicher, C. W., Jr.; Partridge, H. *Chem. Phys. Lett.* **1995**, *240*, 533.

(19) Martin, J. M. L.; Uzan, O. *Chem. Phys. Lett.* **1998**, *282*, 16.

(20) Dunning, T. H., Jr.; Peterson, K. A.; Wilson, A. K. *J. Chem. Phys.* **2001**, *114*, 9244.

(21) (a) Bartlett, R. J. *Annu. Rev. Phys. Chem.* **1981**, *32*, 359. (b) Raghavachari, K.; Trucks, G. W.; Pople, J. A.; Head-Gordon, M. *Chem. Phys. Lett.* **1989**, *157*, 479. (c) Olsen, J.; Jorgensen, P.; Koch, H.; Balkova, A.; Bartlett, R. J. *J. Chem. Phys.* **1996**, *104*, 8007.

(22) (a) Krishnan, R.; Binkley, J. S.; Seeger, R.; Pople, J. A. *J. Chem. Phys.* **1980**, *72*, 650. (b) McLean, A. D.; Chandler, G. S. *J. Chem. Phys.* **1980**, *72*, 5639. (c) Clark, T.; Chandrasekhar, J.; Spitznagel, G. W.; Schleyer, P. v. R. *J. Comput. Chem.* **1983**, *4*, 294. (d) Frisch, M. J.; Pople, J. A.; Binkley, J. S. *J. Chem. Phys.* **1984**, *80*, 3265.

(23) Møller, C.; Plesset, M. S. *Phys. Rev.* **1934**, *46*, 618.

(24) (a) Siegbahn, P. E. M.; Almlöf, J.; Heiberg, A.; Roos, B. O. *J. Chem. Phys.* **1981**, *74*, 2384. (b) Roos, B. O.; Taylor, P. R.; Siegbahn, P. E. M. *Chem. Phys.* **1980**, *48*, 157.

(25) Ochterski, J. W.; Petersson, G. A.; Montgomery, J. A., Jr *J. Chem. Phys.* **1996**, *104*, 2598.

(26) (a) Martin, J. M. L.; de Oliveira, G. *J. Chem. Phys.* **1999**, *111*, 1843. (b) Parthiban, S.; Martin, J. M. L. *J. Chem. Phys.* **2001**, *114*, 6014.

(27) Frisch, M. J.; Trucks, G. W.; Schlegel, H. B.; Scuseria, G. E.; Robb, M. A.; Cheeseman, J. R.; Montgomery, J. A., Jr.; Vreven, T.; Kudin, K. N.; Burant, J. C.; Millam, J. M.; Iyengar, S. S.; Tomasi, J.; Barone, V.; Mennucci, B.; Cossi, M.; Scalmani, G.; Rega, N.; Petersson, G. A.; Nakatsuji, H.; Hada, M.; Ehara, M.; Toyota, K.; Fukuda, R.; Hasegawa, J.; Ishida, M.; Nakajima, T.; Honda, Y.; Kitao, O.; Nakai, H.; Klene, M.; Li, X.; Knox, J. E.; Hratchian, H. P.; Cross, J. B.; Bakken, V.; Adamo, C.; Jaramillo, J.; Gomperts, R.; Stratmann, R. E.; Yazyev, O.; Austin, A. J.; Cammi, R.; Pomelli, C.; Ochterski, J. W.; Ayala, P. Y.; Morokuma, K.; Voth, G. A.; Salvador, P.; Dannenberg, J. J.; Zakrzewski, V. G.; Dapprich, S.; Daniels, A. D.; Strain, M. C.; Farkas, O.; Malick, D. K.; Rabuck, A. D.; Raghavachari, K.; Foresman, J. B.; Ortiz, J. V.; Cui, Q.; Baboul, A. G.; Clifford, S.; Cioslowski, J.; Stefanov, B. B.; Liu, G.; Liashenko, A.; Piskorz, P.; Komaromi, I.; Martin, R. L.; Fox, D. J.; Keith, T.; Al-Laham, M. A.; Peng, C. Y.; Nanayakkara, A.; Challacombe, M.; Gill, P. M. W.; Johnson, B.; Chen, W.; Wong, M. W.; Gonzalez, C.; Pople, J. A. *Gaussian 03, Revision D.01*; Gaussian, Inc.: Wallingford, CT, 2004.

(28) (a) *MOLEKEL 4.3*; Flükiger, P.; Lüthi, H. P.; Portmann, S.; Weber, J. Swiss Center for Scientific Computing; Manno, Switzerland, 2000−2002. (b) Portmann, S.; Lüthi, H. P. *Chimia* **2000**, *54*, 766.

(29) (a) Berkowitz, J.; Marquart, J. R. *J. Chem. Phys.* **1963**, *39*, 275. (b) Berkowitz, J.; Lifshitz, C. *J. Chem. Phys.* **1968**, *48*, 4346. (c) Berkowitz, J. *J. Chem. Phys.* **1975**, *62*, 4074. (d) Meyer, B. *Chem. Rev.* **1976**, *76*, 367. (e) Rosinger, W.; Grade, M.; Hirschwald, W. *Ber. Bunsen-Ges. Phys. Chem.* **1983**, *87*, 536.

(30) (a) Rice, J. E.; Amos, R. D.; Handy, N. C.; Lee, T. J.; Schaefer, H. F.; III, *J. Chem. Phys.* **1986**, *100*, 7847. (b) Raghavachari, K.; Rolfing, C. M.; Binkley, J. S. *J. Chem. Phys.* **1990**, *93*, 5862. (c) Koch, W.; Natterer, J.; Heinemann, C. *J. Chem. Phys.* **1995**, *102*, 6159. (d) Goddard, J. D.; Chen, X.; Orlova, G. *J. Phys. Chem. A* **1999**, *103*, 4078. (e) Millefiori, S.; Alparone, A. *J. Phys. Chem. A* **2001**, *105*, 9489. (f) Thorwirth, S.; McCarthy, M. C.; Gottlieb, C. A.; Thaddeus, P.; Gupta, H.; Stanton, J. F. *J. Chem. Phys.* **2005**, *123*, 054326. (g) Azizi, Z.; Roos, B. O.; Veryazov, V. *Phys. Chem. Chem. Phys.* **2006**, *8*, 2727. (h) Peterson, K. A.; Lyons, J. R.; Francisco, J. S. *J. Chem. Phys.* **2006**, *125*, 084314.

(31) McCarthy, M. C.; Thorwirth, S.; Gottlieb, C. A.; Thaddeus, P. *J. Am. Chem. Soc.* **2004**, *126*, 4096.

(32) (a) Toscano, M.; Russo, N.; Rubio, J. *J. Chem. Soc., Faraday Trans.* **1996**, *92*, 2681. (b) Minerva, T.; Russo, N.; Sicilia, E.; Toscano, M. *J. Chem. Soc., Faraday Trans.* **1997**, *93*, 3309. (c) Wong, M. W.; Chwee, T. S.; Steudel, R. *J. Phys. Chem. A* **2004**, *108*, 7091.

(33) Chase, M. W. NIST-JANAF Themochemical Tables, 4th ed *J. Phys. Chem. Ref. Data* **1998**, 1−1951; Monograph 9.

(34) *NIST Chemistry WebBook, NIST Standard Reference Database Number 69*; Linstrom, P. J., Mallard, W. G., Eds.; 2005.

(35) Sansonetti, J. E.; Martin, W. C.; Young, S. L. *Handbook of Basic Atomic Spectroscopic Data*; National Institute of Standards and Technology: Gaithersburg, MD, 2006.

(36) Hunsicker, S.; Jones, R. O.; Gantefor, G. *J. Chem. Phys.* **1995**, *102*, 5197.

(37) Meredith, C.; Quelch; G, E.; Schaefer, H. F., III *J. Am. Chem. Soc.* **1991**, *113*, 1186.

(38) (a) Frank, A. J.; Sadílek, M.; Ferrier, J. G.; Tureček, F. *J. Am. Chem. Soc.* **1996**, *118*, 11321. (b) Goumri, A.; Rocha, J-D. R.; Laakso, D.; Smith, C. E.; Marshall, P. *J. Phys. Chem. A* **1999**, *103*, 11328. (c) Blitz, M. A.; Hughes, K. J.; Pilling, M. J.; Robertson, S. H. *J. Phys. Chem. A* **2006**, *110*, 2996. (d) Ballester, M. Y.; Varandas, A. J. C. *Chem. Phys. Lett.* **2007**, *433*, 279.

(39) (a) Martin, J. D. D.; Hepburn, J. W. *J. Chem. Phys.* **1998**, *109*, 8139. (b) Caldwell, G.; Renneboog, R.; Kebarle, P. *Can. J. Chem.* **1989**, *67*, 661.

JP8055637